



Despite this long history, little is known about the connection between folding of the protein and assembly of the dimetal site. The relatively small size of the Hr subunit and the "spontaneous self-assembly" of synthetic complexes which mimic the diiron site structure<sup>8</sup> suggest that folding of the protein subunit into the "four-helix bundle" and assembly of its diiron site (cf. Chart I) could be interrelated. Our initial efforts to delineate this relationship led to the first successful reconstitution of the diiron site in Hr from the apoprotein and iron(II) salts.<sup>9</sup> This reconstitution regenerated a functional protein. We have set out to incorporate other metals into Hr in place of iron in order to further probe the aforementioned relationship. Cobalt(II) has often been substituted into metal sites of proteins which contain O,N ligands.<sup>10</sup> Co(II) substitution provides useful spectroscopic probes which can be used to delineate the coordination chemistry and reactivity of metal sites in proteins. Complexes containing a ( $\mu$ -hydroxo)bis( $\mu$ -carboxylato)dicobalt core analogous to the diiron site structure in Hr have been synthesized,<sup>11</sup> but such a dicobalt site has not been found in any living system. Here we report results supporting the achievement of Co(II) substitution at the diiron site of Hr using a method analogous to that reported previously for reconstitution with iron.<sup>9</sup>

### Experimental Section

**Materials and Methods.** Chemicals were purchased from Baker, Sigma, Bio-Rad, Pharmacia, and BDH Ltd. at the highest available purities. Live specimens of *Phascolopsis gouldii* were obtained from the Marine Biological Laboratory, Woods Hole, MA. MetHr was isolated and purified from coelomic hemerythrocytes of these organisms by a previously described procedure,<sup>12</sup> except that the crystallization step was sometimes omitted. The concentration of metHr was determined at pH 7.0 by measuring absorbance at 355 nm ( $\epsilon_{2Fe} = 6400 \text{ M}^{-1} \text{ cm}^{-1}$ ).<sup>13</sup> ApoHr was prepared as described previously,<sup>9</sup> and its concentration was estimated by assuming a 100% yield from the starting metHr. All solutions were prepared in deionized water. Unless otherwise specified, the buffer was 50 mM HEPES, pH 7.0. All anaerobic operations were performed under Ar in septum-capped vials connected to a vacuum manifold by hypodermic needles. Solutions were made anaerobic by several cycles of evacuation and flushing with Ar. Liquids and solutions were transferred via gastight syringe. A 2.5- $\times$  25-cm Sephadex G-25 gel filtration column was made anaerobic by passage of 100 mL of anaerobic buffer containing 10 mM sodium dithionite followed by sufficient buffer to remove the sodium dithionite. This removal was monitored by absorbance of the eluate at 315 nm. All operations were carried out at room temperature except for that of concentrating protein solutions in the Amicon cell, which was carried out at 4 °C.

**Preparation of Cobalt-Substituted Hr.** To an anaerobic solution of ~300 mM 2-mercaptoethanol in 1 mL of buffer was added 5–8 mg of cobalt(II) nitrate hexahydrate under a stream of Ar. A clear green solution was thus obtained. This cobalt stock solution and the solution of apoHr were freshly prepared for each reaction. One milliliter of ~0.2 mM apoHr in buffer containing 6 M guanidinium chloride was made

anaerobic in a 2-dram vial. A 10–15- $\mu$ L volume of 2-mercaptoethanol and then 0.2 mL of the Co(II) stock solution were added to the apoHr solution in a dropwise fashion, mixing the solution after the addition of each drop. The cobalt/Hr subunit ratio after addition was in the range 8–14 and the 2-mercaptoethanol concentration was in the range 160–220 mM. The resulting solution was slowly diluted with anaerobic buffer to a total volume of 5 mL, at a rate of ~1 mL/30 min. After dilution the greenish solution was spun in a clinical centrifuge and the supernatant was loaded onto the anaerobic 2.5- $\times$  25-cm Sephadex G-25 column and eluted with anaerobic buffer. The cobalt-substituted Hr eluted as the first band, as monitored by absorbance at 280 nm. A sample of cobalt-substituted Hr for X-ray absorption spectroscopy was prepared by concentrating the eluted protein in an Amicon cell under Ar to ~4 mM in Hr subunits in a final volume of 0.3 mL while the buffer was changed to 50 mM phosphate containing 150 mM sodium sulfate at pH 7.0 by repeated dilutions and reconcentrations. The cobalt-substituted Hr was found to be somewhat more soluble in this latter buffer than in HEPES.

**Analytical Methods.** Total protein concentrations in preparations of cobalt-substituted Hr were determined using the Bio-Rad protein assay with native metHr as the protein standard. MetHr concentration was determined using the extinction coefficient listed above. Metal contents of the cobalt-substituted Hr were obtained by inductively coupled plasma emission spectrometry on a Jarrell-Ash Atomcomp 965 spectrometer. Approximately 1 mg/mL of protein solutions were used with the protein buffers (50 mM HEPES, pH 7.0) serving as blank samples. Electronic absorption extinction coefficients of cobalt-substituted Hr (Table I) were calculated from the protein concentrations as determined from the Bio-Rad assay, the cobalt analysis, and the measured electronic absorbances of the same protein solutions.

Analytical gel filtration was used to determine the molecular weight of cobalt-substituted Hr. The chromatography was performed at room temperature on a 1.6- $\times$  50-cm Superose 12 preparative grade column equilibrated with 10 mM phosphate at pH 7.5 containing 150 mM sodium sulfate and running at a flow rate of 0.2 mL/min. A concentration of ~1 mM in Hr subunits in a volume of less than 0.4 mL was applied to the column. Absorbance of the eluate was monitored at 280 nm. MetHr ( $M_r \sim 108\,000$ ) and metmyoHr iso I ( $M_r \sim 13\,800$ ),<sup>14</sup> both from *P. gouldii*, served as molecular weight standards.

**Spectroscopic Measurements. Electronic Absorption.** UV/vis spectra were obtained on either a Perkin-Elmer 554 spectrophotometer or a Perkin-Elmer Model 3840 lambda array spectrophotometer. Quartz cells of 1-cm path length were used. Near-IR spectra were obtained on an OLIS 4000c spectrophotometer using a cell with a 1-mm path length. Cobalt-substituted Hr concentrations were 2–4 mM in Hr subunits for visible and near-IR measurements.

**CD.** Far-UV CD spectra were obtained on a Jasco J-500c spectropolarimeter interfaced to an IBM PC-XT computer. The instrument was calibrated using a standard androstereone solution. Protein samples of ~0.5 mg/mL (~40  $\mu$ M in Hr subunits) were used in a 0.01-cm path length quartz cell. Molar ellipticity,  $[\theta]$ , was calculated from the equation<sup>15</sup>

$$[\theta] = 100\theta^\circ / lc$$

where  $\theta^\circ$  is the measured rotation in degrees,  $l$  is the optical path length in centimeters, and  $c$  is the protein concentration expressed as amino acid residue molarity. Peptide helix contents for the native and reconstituted Hrs were calculated from the molar ellipticity at 222 nm using  $[\theta]_{222} = -35\,000 \text{ deg cm}^2/\text{dmol} + 3000 \text{ deg cm}^2/\text{dmol}$  for 100% helix and 0% helix, respectively.<sup>16</sup> Near-IR CD spectra were obtained at room temperature on a Jasco J-730 spectropolarimeter interfaced to an IBM PS/2 computer. A 1-cm path length quartz cell was used with concentrations of 2–3 mM in Hr subunits in 50 mM phosphate containing 150 mM sodium sulfate at pH 7.0. A buffer background (which had no distinct features) was subtracted from the protein spectrum. The CD scale was transformed to  $\Delta A$  from the measured ellipticity,  $\theta^\circ$  in degrees, using  $\Delta A = 3.0 \times 10^{-2}\theta^\circ$ . The anisotropy factor,  $\Delta A/A$ , is normally calculated using the absorbance,  $A$ , of the sample at the same wavelength used to calculate  $\Delta A$ .<sup>17</sup>

**X-ray Absorption.** Fluorescence data were collected at station C-2 of the Cornell High Energy Synchrotron Source (CHESS) on a frozen

- Abbreviations used: Hr, hemerythrin; HEPES, 4-(2-hydroxyethyl)-1-piperazineethanesulfonate; CD, circular dichroism; acac, acetylacetonate; EXAFS, extended X-ray absorption fine structure; MES, N-morpholineethanesulfonic acid;  $M_r$ , relative molecular mass; Im, imidazole; MTACN, 1,4,7-trimethyl-1,4,7-triazacyclononane.
- Holmes, M. A.; Le Trong, I.; Turley, S.; Sieker, L. C.; Stenkamp, R. E. *J. Mol. Biol.* **1991**, *218*, 583–593.
- Wilkins, R. G.; Harrington, P. C. *Adv. Inorg. Biochem.* **1983**, *5*, 51–85.
- Kurtz, D. M., Jr.; Klotz, I. M. *Acc. Chem. Res.* **1984**, *16*, 17–22.
- Kurtz, D. M., Jr. in *O<sub>2</sub> Carriers in Blood and Tissues. Advances in Environmental and Comparative Physiology*; Mangum, C. P., Ed.; Springer-Verlag: New York, 1992; Vol. 13, in press.
- Sanders-Loehr, J. In *Iron Carriers and Iron Proteins*; Loehr, T. M., Ed.; VCH: New York, 1989; pp 373–466.
- (a) Andrews, E. A. *J. Hopkins Univ. Circ.* **1890**, *9*, 65. (b) Klotz, I. M.; Klotz, T. A. *Science* **1955**, *121*, 477–480.
- Kurtz, D. M., Jr. *Chem. Rev.* **1990**, *90*, 585–606.
- Zhang, J.-H.; Kurtz, D. M., Jr.; Xia, Y.-M.; Debrunner, P. G. *Biochemistry* **1991**, *30*, 583–589.
- Bertini, I.; Luchinat, C. *Adv. Inorg. Biochem.* **1984**, *6*, 71–111.
- Chaudhuri, P.; Querbach, J.; Wiegardt, K. *J. Chem. Soc., Dalton Trans.* **1990**, 271–278.
- Bonomi, F.; Long, R. C.; Kurtz, D. M., Jr. *Biochim. Biophys. Acta* **1989**, *999*, 147–156.
- Garbett, K.; Darnall, D. W.; Klotz, I. M.; Williams, R. J. P. *Arch. Biochem. Biophys.* **1969**, *135*, 419–434.

- Zhang, J.-H.; Long, R. C.; Kurtz, D. M., Jr.; Negri, A.; Tedeschi, G.; Bonomi, F. *J. Inorg. Biochem.* **1991**, *43*, 537.
- Darnall, D. W.; Garbett, K.; Klotz, I. M.; Aktipis, S.; Keresztes-Nagy, S. *Arch. Biochem. Biophys.* **1969**, *133*, 103–107.
- (a) Ghadiri, M. R.; Choi, C. *J. Am. Chem. Soc.* **1990**, *112*, 1630–1632. (b) Lyu, P. C.; Marky, L. A.; Kallenbach, N. R. *J. Am. Chem. Soc.* **1989**, *111*, 2733–2734.
- Johnson, M. K. In *Physical Methods in Bioinorganic Chemistry*; Que, L., Jr., Ed.; University Science Books: New York, in press.

solution of cobalt-substituted Hr held near 77 K in a liquid N<sub>2</sub>-filled cryostat. Sample integrity was judged by visual inspection, examination of the edge spectra obtained on sequential scans, and measurement of the electronic absorption spectrum of the sample before and after exposure to synchrotron radiation. None of these criteria revealed any change in the sample during data collection. The beamline was equipped with a Si(111) double-crystal monochromator (resolution ~1 eV), which was detuned by 50% to improve harmonic rejection. The monochromator was calibrated using the first inflection of the *k*-edge of Co foil ( $E = 7.7095$  keV). A large solid angle fluorescence detector<sup>18</sup> equipped with a Mn filter and Soller slits was used in data collection. Data on the model compound Co(acac)<sub>3</sub>,<sup>19</sup> were collected in the transmission mode at room temperature on a powdered sample, diluted with boron nitride to minimize thickness effects.

The pre-edge region of the X-ray absorption spectra of the protein and the model compound were analyzed using a procedure that involves normalization of the edge jump followed by subtraction of the background and edge region with a function composed of linear and arctangent components.<sup>20</sup>

An arbitrary edge energy of 7.723 eV was adopted for the purpose of analyzing the EXAFS spectra of cobalt-substituted Hr and Co(acac)<sub>3</sub>. Data reduction and least-squares fits employing a single-scattering model were performed as described elsewhere in detail,<sup>21</sup> using theoretical phase and amplitude functions from the calculations of McHale et al.<sup>22</sup> and the restricted-fit strategy for minimizing correlations between parameters and the number of independently adjustable parameters used in the least-squares fits.<sup>21</sup> The theoretical phase and amplitude parameters were adjusted using empirical parameters, including an amplitude reduction factor, and an edge energy shift,  $\Delta E$ . Values for these parameters were obtained from fits of the EXAFS spectrum of Co(acac)<sub>3</sub> for first coordination sphere N,O scattering atoms and for second and third coordination sphere C scattering atoms. Values for the amplitude reduction factor and  $\Delta E$  for a Co scattering atom were estimated from parameters previously obtained from a dinuclear Ni complex, bis(2-mercaptoethyl) sulfide.<sup>23</sup> The values of  $\Delta\sigma^2$  reported in Tables II and III are the difference between the values of  $\sigma^2$  obtained in the fit and the value of  $\sigma^2$  for the model compound used to obtain empirical parameters for that absorber-scatterer pair.

Fits were initially generated using Fourier-filtered data, and these fits were subsequently used as initial parameters in the refinement of the model against unfiltered data. All least-squares refinements employed *k*<sup>3</sup>-weighted EXAFS data and minimized  $R = [\sum k^6(x_c - \chi)^2/n]^{1/2}$ , where the summation was performed over the *n* data points collected between 2 and 14 Å<sup>-1</sup>. Although the data beyond  $k = 12$  Å<sup>-1</sup> were quite noisy, the higher *k* data were included in the reported fits in order to maximize the contribution to the EXAFS spectrum from the Co-Co absorber-scatterer pair and to improve the resolution of this shell from the third-shell C scattering atoms. Fits obtained for data truncated at  $k = 12.5$  Å<sup>-1</sup> do not exhibit substantial differences in any of the distances found. The differences between distances obtained from EXAFS analysis and those obtained from crystallography on small model complexes represent good estimates of the errors in the distances obtained from EXAFS analysis. These estimated errors are 0.02 Å for the first coordination sphere atoms and 0.03 Å for the Co-Co distance.<sup>21</sup> Distances obtained for second and third coordination sphere C atoms are not corrected for multiple scattering effects expected for histidine imidazole ligation,<sup>24</sup> and therefore, reported values of *r* are estimates of the actual distances and the values of *N* determined are not accurate estimates of the actual number of C atoms involved.

## Results and Discussion

### I. Preparation of and Analytical Data for Cobalt-Substituted Hr.

**A. Preparation.** The procedure described in the Experimental Section is essentially the same as that used to reconstitute Hr with

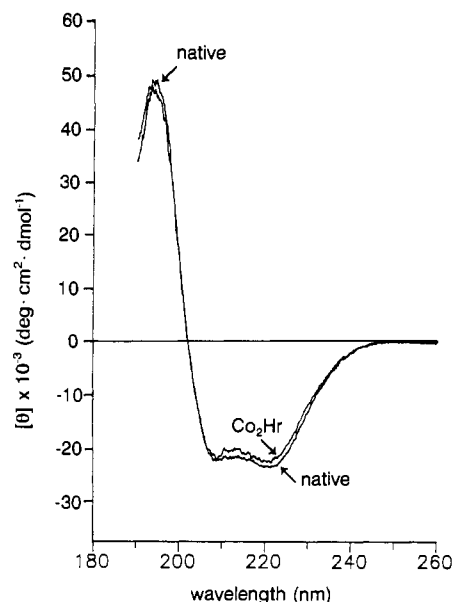


Figure 1. Far-UV CD spectra of metHr (native) and cobalt-substituted Hr (Co<sub>2</sub>Hr) in 50 mM HEPES at pH 7.0.

iron,<sup>9</sup> except that the metal stock solution contained Co(II) instead of Fe(II). The Co(II) stock solution (which also contained 2-mercaptoethanol) was found to be extremely air-sensitive, and this stock solution was, therefore, prepared immediately before reaction with apoHr. Due to this air-sensitivity, all subsequent steps were conducted anaerobically. As is the case for reconstitution with iron, the slow dilution of the apoHr solution in 6 M guanidinium chloride after introduction of the Co(II) was found to be critical for avoidance of protein precipitation. In fact, since *P. gouldii* apoHr is soluble to only about 1.5 μM in subunits in the HEPES buffer without denaturants,<sup>25</sup> a good qualitative indicator of successful reconstitution is a soluble protein product. An anaerobic gel filtration column was used to separate the cobalt-substituted Hr from the extra reagents. After this step, the protein product, which had a light pink color, could be handled in air with no observable changes. The yields of cobalt-substituted Hr, calculated from the protein product concentrations (measured using the Bio-Rad assay) and the starting metHr concentrations, averaged ~50% for multiple preparations. The cobalt-substituted Hr was found to be nearly as stable as metHr in either HEPES or phosphate buffers at pH 7. The cobalt-substituted Hr could be stored frozen at -80 °C, with no significant decomposition upon thawing. Storage of the cobalt-substituted Hr at lower pH, such as in MES buffer at pH 6, for several days at 4 °C resulted in gradual formation of a white precipitate that would not redissolve in the pH 7 HEPES or phosphate buffers. Since apoHr is similarly insoluble in such buffers, the slow precipitation at acidic pH is attributed to loss of cobalt.

**B. Protein and Metal Analyses.** The apoHr solutions used for reconstitutions with cobalt showed only trace amounts of metals, at levels that were no higher than those in the buffered 6 M guanidinium chloride. Total protein and metal analyses of three preparations of cobalt-substituted Hr showed an average of  $1.94 \pm 0.03$  Co/Hr subunit. No iron or other metals were found in the cobalt-substituted protein samples at levels significantly above background. Thus, these metal and protein analyses indicate that iron has been stoichiometrically replaced by cobalt in cobalt-substituted Hr. Dialysis of the cobalt-substituted Hr in 50 mM phosphate and 150 mM sodium sulfate at pH 7.0 against a ~200-fold molar excess of EDTA in the same buffer overnight at 4 °C resulted in no change in the UV-vis spectrum (vide infra) and no protein precipitation. This result indicates that the cobalt in cobalt-substituted Hr is not adventitiously bound to the surface of the protein.

(18) Stern, E. A.; Heald, S. M. *Rev. Sci. Instrum.* **1979**, *50*, 1579-1582.

(19) Hon, P. K.; Pfluger, C. E. *J. Coord. Chem.* **1973**, *3*, 67-71.

(20) Roe, A. L.; Schneider, D. J.; Mayer, R. J.; Pyrz, J. W.; Widom, J.; Que, L., Jr. *J. Am. Chem. Soc.* **1984**, *106*, 1676-1681.

(21) Scarrow, R. C.; Maroney, M. J.; Palmer, S. M.; Que, L., Jr.; Roe, A. L.; Salowe, S. P.; Stubbe, J. *J. Am. Chem. Soc.* **1987**, *109*, 7857-7864.

(22) McHale, A. G.; Veal, B. W.; Paulikas, A. P.; Chan, S.-K.; Knapp, G. S. *J. Am. Chem. Soc.* **1988**, *110*, 3763-3768.

(23) (a) Barclay, G. A.; McPartlin, E. M.; Stephenson, N. C. *Acta Crystallogr.* **1969**, *B25*, 1262-1273. (b) Baker, D. J.; Goodall, D. C.; Moss, D. S. *J. Chem. Soc., Chem. Commun.* **1969**, 325. (c) Maroney, M. J.; Colpas, G. J.; Bagyinka, C.; Baidya, N.; Mascharak, P. K. *J. Am. Chem. Soc.* **1991**, *113*, 3962-3972.

(24) Strange, R. W.; Blackburn, N. J.; Knowles, P. F.; Hasnain, S. S. *J. Am. Chem. Soc.* **1987**, *109*, 7157-7170.

(25) He, Z.-Q.; Kurtz, D. M., Jr. Unpublished results.

**Table I.** UV, Visible and Near-IR Absorption Features of Co<sub>2</sub>Hr<sup>a</sup>

$\lambda$ , nm	$\epsilon$ , M <sup>-1</sup> cm <sup>-1</sup> <sup>b</sup>	$\lambda$ , nm	$\epsilon$ , M <sup>-1</sup> cm <sup>-1</sup> <sup>b</sup>
280	29000	545 (sh)	~60
~320 (sh)	~90	628	~23
500 (sh)	~60	~860	~15
519	68		

<sup>a</sup> Buffer is 50 mM phosphate, 150 mM sodium sulfate at pH 7.0.  
<sup>b</sup> Per 2 Co. Values were determined as described in the Experimental Section.

**C. Protein Secondary Structure and Molecular Weight.** The far-UV CD spectrum of the cobalt-substituted Hr (cf. Figure 1) very closely resembles that of native metHr recorded under the same conditions. The spectrum of native metHr in Figure 1 is itself essentially identical to the previously published CD spectrum of this protein.<sup>15</sup> The abscissa is presented as residue molar ellipticity with the values calculated from protein concentrations using  $\epsilon_{355}$  for metHr and  $\epsilon_{280}$  for cobalt-substituted Hr (Table I). The double minima at 208 and 222 nm are characteristic of proteins with a large percentage of helix content,<sup>16</sup> consistent with the "four-helix bundle" structure shown in Chart I. For proteins with predominantly helical secondary structure,  $[\theta]_{222}$  can be used to quantitate the percentage helix content using the values for 100% and 0% helix listed in the Experimental Section.<sup>16</sup> The average values for two determinations each were  $[\theta]_{222} = 23\,655$  deg cm<sup>2</sup>/dmol for metHr and 22 463 deg cm<sup>2</sup>/dmol for cobalt-substituted Hr, which translates to 70 and 67% helix contents, respectively. The X-ray crystal structures of octameric Hrs from *P. gouldii*, the organism used in this work, and from *Themiste dyscritum* both show ~70% of the amino acid residues residing in helical regions.<sup>26,27</sup> The close similarities in both the shape of the spectra and  $[\theta]_{222}$  between metHr and cobalt-substituted Hr strongly suggest that the four-helix bundle structure is retained in cobalt-substituted Hr.

Analytical gel filtration chromatography showed that cobalt-substituted Hr elutes as a single band at a volume of 49 mL from a 1.6- × 50-cm Superose 12 gel filtration column. This elution volume was identical within experimental error to that of native *P. gouldii* metHr (48.7 mL) and was quite different from the elution volume of *P. gouldii* metmyoHr iso I (65 mL). This result shows that essentially all of the cobalt-substituted Hr is octameric and rules out the presence of any significant proportion of a monomeric form.

The preceding results strongly suggest that the cobalt-substituted Hr has a structure essentially identical to that of native Hr except that the diiron site in the native protein has been replaced by a dicobalt site. The cobalt-substituted Hr is, therefore, referred to as Co<sub>2</sub>Hr in the subsequent discussion, which presents additional evidence supporting this conclusion.

**II. Spectroscopy and Structure of the Cobalt Centers.** The fairly reducing conditions used to prepare Co<sub>2</sub>Hr should result in insertion of Co(II), as is almost invariably the case for other cobalt-substituted proteins.<sup>28</sup> Added oxidants such as hydrogen peroxide are necessary to obtain Co(III) in proteins; O<sub>2</sub> from air is usually insufficient.<sup>29</sup> However, given the O<sub>2</sub>-carrying function of the native protein, we sought direct spectroscopic evidence for the oxidation state(s) of cobalt in Co<sub>2</sub>Hr. Unless otherwise noted, all spectroscopic measurements were performed on solutions that had been exposed to air.

**A. UV/Vis and Near-IR Absorption.** The UV, visible, and near-IR absorption spectral characteristics of Co<sub>2</sub>Hr are shown in Figure 2 and summarized in Table I. The absorption band at 280 nm (not shown in Figure 2) is due primarily to the two tryptophan and five tyrosine residues in *P. gouldii* Hr.<sup>26</sup> A shoulder at ~320 nm on the low-energy side of the 280-nm band is barely discernible in Figure 2. This absorption and those

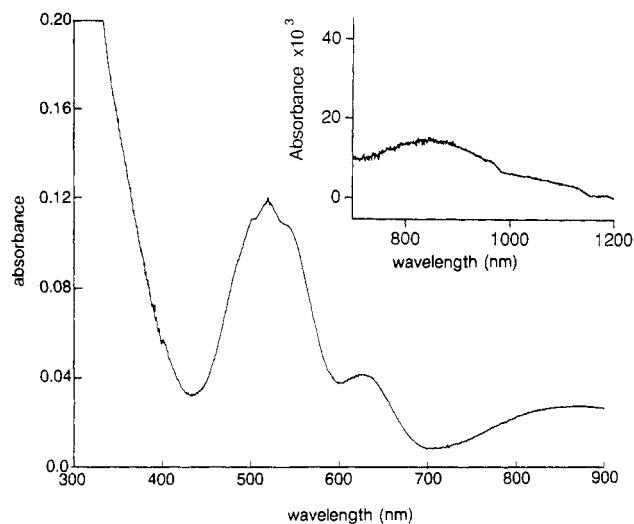


**Figure 2.** Visible and near-IR (inset) absorption spectra of Co<sub>2</sub>Hr in 50 mM phosphate and 150 mM sodium sulfate at pH 7.0.

remaining in Figure 2 and Table I are presumably due to the cobalt centers, since they are not observed in any other known derivative of Hr.

The visible and near-IR regions of the absorption spectrum are quite informative with respect to oxidation and spin states and coordination spheres of the cobalt centers. The absorption spectrum of Co<sub>2</sub>Hr in the region between 350 and 1000 nm consists of at least five discernible features. The highest absorbing feature in this region is at 519 nm with a molar extinction coefficient  $\epsilon_{Co} = 34$  M<sup>-1</sup> cm<sup>-1</sup>. Both the absorption maxima and extinction coefficients in Figure 2 and Table I are inconsistent with the presence of Co(III), whose complexes of N,O donor ligands (the most likely ligands in Co<sub>2</sub>Hr) typically show two or more d-d transitions but only within the ranges ~350–600 nm and  $\epsilon_{Co} \sim 75$ –150 M<sup>-1</sup> cm<sup>-1</sup>.<sup>30a</sup> The preceding statement also applies to dicobalt(III) and mixed-valence dicobalt(II,III) complexes having a ( $\mu$ -hydroxo)bis( $\mu$ -carboxylato)dicobalt core and terminal nitrogen donor ligands.<sup>11</sup> This core structure is a likely possibility for a dicobalt site in Co<sub>2</sub>Hr, given the analogous structure for the diiron(II) site in deoxyHr.<sup>2</sup> The absorption spectrum of Co<sub>2</sub>Hr does not resemble those of the ( $\mu$ -peroxo/superoxo)dicobalt(III) complexes which result from reactions of Co(II) complexes with O<sub>2</sub>.<sup>30b</sup> Finally, the features of the spectrum in Figure 2 are unaffected by anaerobic addition of excess sodium dithionite at pH 7. These observations strongly support the conclusion that most or all of the cobalt in Co<sub>2</sub>Hr is Co(II), even in the presence of air. The X-ray absorption results (vide infra) provide additional support for this conclusion.

Assuming that high-spin Co(II) is the only remaining possibility in Co<sub>2</sub>Hr,<sup>31</sup> the spectral data in Figure 2 and Table I rule out tetrahedral or pseudotetrahedral coordination, which results in much more intense absorptions ( $\epsilon_{Co}$  of 200–800 M<sup>-1</sup> cm<sup>-1</sup>) with maxima between 550 and 650 nm for an N,O ligand donor set.<sup>28,30a</sup> The molar extinction coefficient for Co<sub>2</sub>Hr at 519 nm is at the high end of the range for high-spin six-coordinate Co(II) with N,O donor ligands ( $\epsilon_{Co} \sim 5$ –40 M<sup>-1</sup> cm<sup>-1</sup>).<sup>28,30a</sup> On the basis of comparisons to similar complexes, the major contributor to the absorption around 519 nm is the  ${}^4T_{1g}(F) \rightarrow {}^4T_{1g}(P)$  transition in  $O_h$  symmetry. The multiple features in this region are not uncommon for six-coordinate Co(II) complexes and can arise from the forbidden two-electron  ${}^4T_{1g}(F) \rightarrow {}^4A_{2g}(F)$  transition and from the lifting of state degeneracies due to lower than  $O_h$  symmetry ligand fields. Deconvolutions of the spectrum of Co<sub>2</sub>Hr using the

(26) Loehr, J. S.; Loehr, T. M. *Adv. Inorg. Biochem.* **1979**, *1*, 235–252.

(27) Holmes, M. A.; Stenkamp, R. E. *J. Mol. Biol.*, in press.

(28) Bertini, I.; Luchinat, C. *Adv. Inorg. Biochem.* **1984**, *6*, 71–111 and references therein.

(29) Van Wart, H. *Meth. Enzymol.* **1988**, 95–110.

(30) Lever, A. B. P. *Inorganic Electronic Spectroscopy*, 2nd ed.; Elsevier: Amsterdam, 1984; pp (a) 457–505, (b) 285–296.

(31) Low-spin Co(II) has been observed in proteins only when square-planar ligands such as porphyrins are present or when strong field ligands such as CN<sup>-</sup> are added.<sup>28</sup> Neither possibility exists for our preparations of Co<sub>2</sub>Hr.

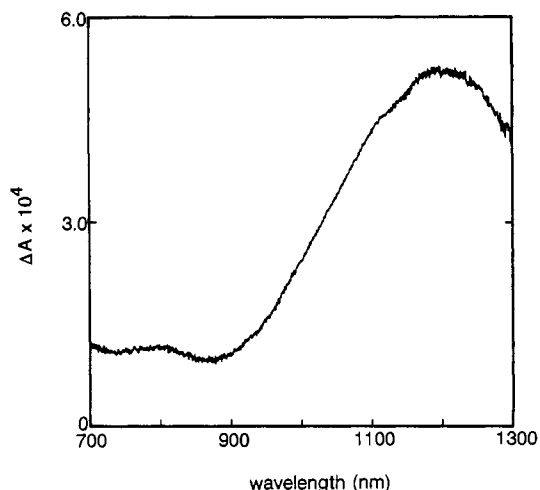


Figure 3. Near-IR CD spectrum of  $\text{Co}_2\text{Hr}$  in 50 mM phosphate and 150 mM sodium sulfate at pH 7.0.

program SP Serv show that the absorption envelope between 400 and 600 nm is best fit by two relatively intense Gaussian components with maxima at  $\sim 497$  and  $555$  nm and a third Gaussian component at  $\sim 520$  nm, which is 1 order of magnitude weaker than the former two components. This weaker component could be due to the forbidden two-electron transition referred to above.

$\text{Co(II)}$ , when substituted in proteins such as conalbumin,<sup>28</sup> glyoxylase I,<sup>28</sup> and iron-activated alcohol dehydrogenase,<sup>32</sup> shows absorption spectra between 400 and 700 nm with shapes and intensities similar to that of  $\text{Co}_2\text{Hr}$ . These other proteins were concluded to contain high-spin  $\text{Co(II)}$  in a pseudooctahedral coordination. However,  $\text{Co}_2\text{Hr}$  shows an additional very broad absorption band at  $\sim 860$  nm, which is lacking in spectra of any of these other proteins. Six-coordinate  $\text{Co(II)}$  complexes with O,N ligands typically show a broad weak band ( $\epsilon_{\text{Co}} \sim 5\text{--}10$ ) between 1000 and 1250 nm due to the  ${}^4\text{T}_{1g}(\text{F}) \rightarrow {}^4\text{T}_{2g}(\text{F})$  transition but no bands between  $\sim 650$  and  $\sim 1000$  nm.<sup>28,30a</sup> This statement also applies to a ( $\mu$ -hydroxo)bis( $\mu$ -carboxylato)dicobalt(II) complex with terminal N-donor ligands.<sup>11</sup> In addition, the spectrum of  $\text{Co}_2\text{Hr}$  shows a clear absorption band at  $\sim 628$  nm, which is either absent or present as a weak shoulder in spectra of six-coordinate  $\text{Co(II)}$  complexes with N,O donor ligands.<sup>11,28,30a</sup> These differences between the absorption spectrum of  $\text{Co}_2\text{Hr}$  and six-coordinate  $\text{Co(II)}$  complexes must arise from some proportion of the  $\text{Co(II)}$  in  $\text{Co}_2\text{Hr}$  having either a severely distorted octahedral coordination or, more likely, five-coordination. In fact, absorption spectra of five-coordinate  $\text{Co(II)}$  complexes with N,O donor ligands do show bands near 860 and 628 nm in addition to a multiply featured band at  $\sim 500$  nm.<sup>28,30a</sup> In  $D_{3h}$  symmetry these three bands have been assigned to  ${}^4\text{A}'_2 \rightarrow {}^4\text{E}'$ ,  ${}^4\text{A}'_2(\text{F}) \rightarrow {}^4\text{A}'_2(\text{P})$ , and  ${}^4\text{A}'_2(\text{F}) \rightarrow {}^4\text{E}''(\text{P})$  transitions, respectively. If both five- and six-coordinate  $\text{Co(II)}$  are present in significant proportions in  $\text{Co}_2\text{Hr}$ , then the 860-nm band (due to the five-coordinate Co) and another weaker band between 1000 and 1250 nm (due to the six-coordinate Co) should both be present in the absorption spectrum. Unfortunately, at the available protein concentrations, the absorption beyond 1000 nm was too weak to provide any useful information on our spectrometer. However, CD spectroscopy can often detect magnetic dipole allowed transitions in this region.

**B. Near-IR CD.** The  ${}^4\text{T}_{1g}(\text{F}) \rightarrow {}^4\text{T}_{2g}(\text{F})$  transition giving rise to the near-IR absorption from the six-coordinate  $\text{Co(II)}$  is predicted to be magnetic dipole allowed, whereas the  ${}^4\text{A}'_2 \rightarrow {}^4\text{E}'$  transition giving rise to the higher energy near-IR absorption from the five-coordinate  $\text{Co(II)}$  is predicted to be magnetic dipole forbidden. These predictions can be tested by CD spectroscopy. Figure 3 shows the near-IR CD spectrum of  $\text{Co}_2\text{Hr}$ . In qualitative agreement with the predicted activities, a broad band is indeed observed with a maximum at  $\sim 1200$  nm, whereas little or no CD

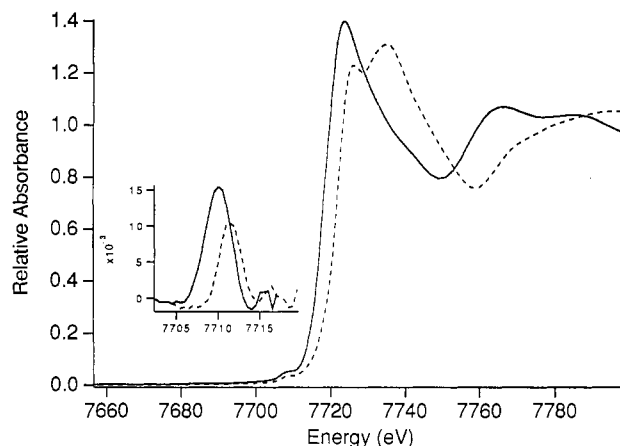


Figure 4. Comparison of the Co  $k$ -edge spectra of  $\text{Co}_2\text{Hr}$  (solid line) and  $\text{Co}(\text{acac})_3$  (dashed line). Inset: Background-corrected pre-edge spectrum showing the  $1s \rightarrow 3d$  transition.

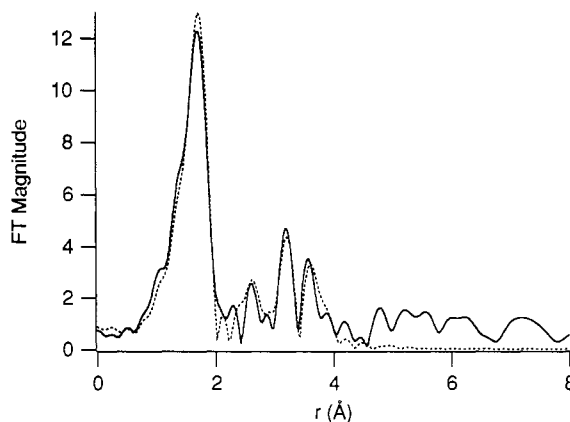


Figure 5. Fourier-transformed EXAFS spectrum of  $\text{Co}_2\text{Hr}$  and the four-shell fit generated to Fourier-filtered data (backtransform window = 1.1–3.8 Å). Numerical data are contained in Table II.

is obtained from the 860-nm absorption. A value for the anisotropy factor (defined in the Experimental Section),  $\Delta A/A > 0.01$ , is often used as a criterion for identifying magnetic dipole allowed transitions.<sup>17,33</sup> A value of  $\Delta A/A > 0.027$  was calculated<sup>34</sup> for the 1200-nm band in Figure 3, which supports its assignment to the magnetic dipole allowed  ${}^4\text{T}_{1g}(\text{F}) \rightarrow {}^4\text{T}_{2g}(\text{F})$  transition of the six-coordinate  $\text{Co(II)}$ . Similarly, a value of  $\Delta A/A = 0.005$  was calculated for the 860-nm band, consistent with its assignment to the magnetic dipole forbidden  ${}^4\text{A}'_2 \rightarrow {}^4\text{E}'$  transition of the five-coordinate  $\text{Co(II)}$ .

**C. X-ray Absorption. 1. Absorption Edge.** The Co  $k$ -edge spectra obtained for  $\text{Co}_2\text{Hr}$  and  $\text{Co}(\text{acac})_3$  are shown in Figure 4. The absorption edge for the  $\text{Co}(\text{acac})_3$  is at a higher energy than that of  $\text{Co}_2\text{Hr}$ , consistent with the assignment of a +II oxidation state for Co in the protein. The electronic absorption spectroscopy rules out four- but not five-coordination for some portion of the  $\text{Co(II)}$  in  $\text{Co}_2\text{Hr}$ . Information from the area under the pre-edge feature assigned to the  $1s \rightarrow 3d$  transition can also be used to determine coordination number/geometry.<sup>20,23c,35,36</sup> This transition is symmetry forbidden in centrosymmetric point groups but gains intensity in noncentrosymmetric point groups due to  $p$ - $d$  mixing. Therefore, this transition increases in area in the order six-coordinate < five-coordinate < four-coordinate

(33) Richardson, F. S. *Chem. Rev.* **1979**, *109*, 17–36.

(34) The value of  $A$  for the 1200-nm CD band was estimated using the absorbance at 862 nm, because we could measure this absorbance more accurately than that at 1200 nm and because the absorbance at 1200 nm is lower than that at 860 nm. Thus, the reported value of  $\Delta A/A$  for the 1200-nm band represents a lower limit.

(35) Maroney, M. J.; Scarrow, R. C.; Que, L., Jr.; Roe, A. L.; Lukat, G. S.; Kurtz, D. M., Jr. *Inorg. Chem.* **1989**, *28*, 1342–1348.

(36) Shiro, Y.; Sato, F.; Suzuke, T.; Iizuka, T.; Matsushita, T.; Oyanagi, H. *J. Am. Chem. Soc.* **1990**, *112*, 2921–2924.

(32) Bakshi, E. N.; Tse, P.; Murray, K. S.; Hanson, G. R.; Scopes, R. K.; Wedd, A. G. *J. Am. Chem. Soc.* **1989**, *111*, 8707–8713.

Table II. EXAFS Fits Refined against Fourier-Filtered Data for Co<sub>2</sub>Hr

backtransform window, Å	no. of scattering atoms	$r$ , Å	$10^3 \Delta \sigma^2$ , Å <sup>2</sup>	correlation coeff > 0.6	$R$
$r = 1.1-2.1$	6	Co-N,O = 2.120 (2)	4.7 (3)		0.61
	5	Co-N,O = 2.118 (1)	3.0 (2)		0.44
	4	Co-N,O = 2.116 (1)	1.4 (2)		0.41
	4	Co-N,O = 2.133 (4)	5.2 (6)	$r_1/r_2 = -0.77$ ; $r_2/\sigma_1 = 0.73$	0.40
	1	Co-N,O = 2.096 (4)	-2.2 (3)	$\sigma_1/\sigma_2 = -0.67$	
	3	Co-N,O = 2.148 (6)	7.2	$r_1/r_2 = -0.76$ ; $r_2/\sigma_1 = 0.78$	0.38
	2	Co-N,O = 2.102 (4)	-0.7		
	2	Co-N,O = 2.178 (10)	11.1 (20)	$r_1/r_2 = -0.66$ ; $r_2/\sigma_1 = 0.80$	0.36
3	Co-N,O = 2.107 (2)	0.2			
$r = 2.1-2.9$	1.9 (2)	Co-C = 3.068 (5)	not varied		0.30
$r = 2.9-3.4$	1	Co-Co = 3.535 (2)	-1.5		0.17
$r = 2.1-4.0$	1.8 (3)	Co-C = 3.056 (9)	not varied		0.51
	1	Co-Co = 3.522 (5)	-0.7		
	4.1 (4)	Co-C = 4.102 (6)	not varied		
$r = 1.1-3.8$	5	Co-N,O = 2.118 (2)	3.1 (3)		0.57
	2.2 (3)	Co-C = 3.058 (8)	not varied		
	1	Co-Co = 3.523 (6)	-0.7		
	4.8 (5)	Co-C = 4.078 (6)	not varied		

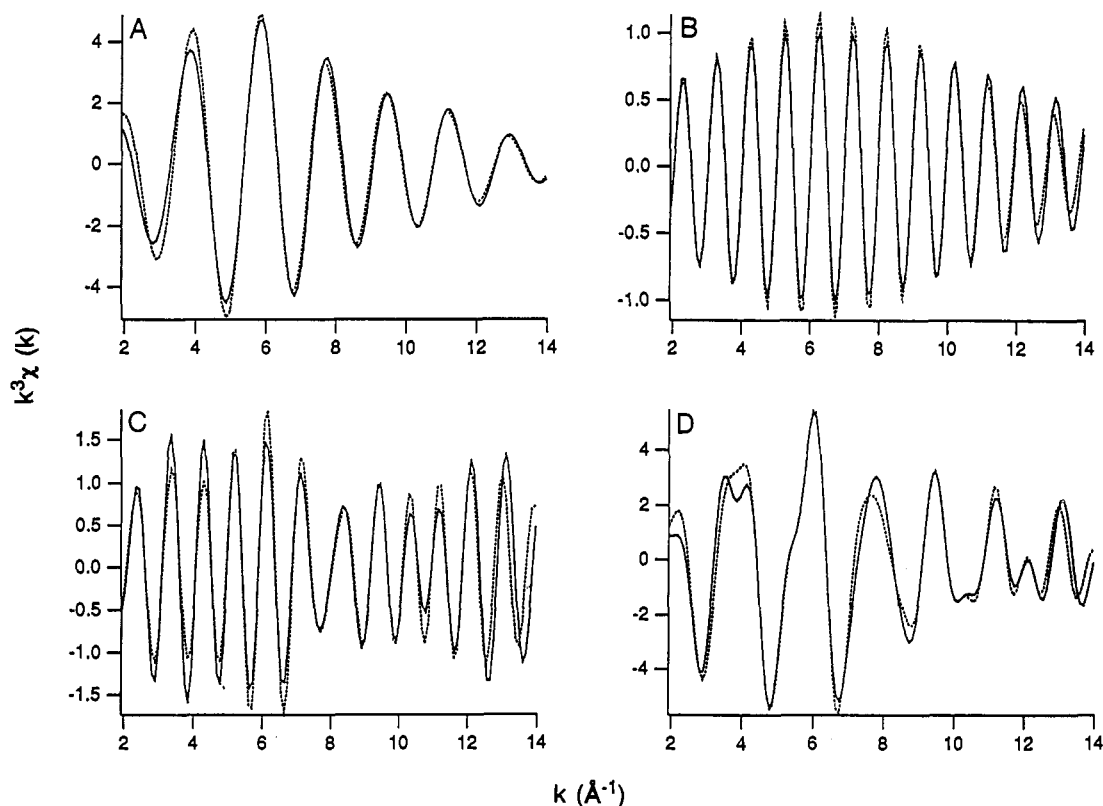


**Figure 6.** Fourier-filtered EXAFS spectra from Co<sub>2</sub>Hr (solid lines) and fits (dashed lines): (A) EXAFS due to first coordination sphere N,O-scattering atoms (backtransform window = 1.1–2.1 Å); (B) EXAFS arising from the Co–Co absorber–scatterer pair (backtransform window = 2.9–3.4 Å); (C) EXAFS arising from second and third coordination sphere atoms and a three-shell fit (backtransform window = 2.1–4.0 Å); (D) Fourier-filtered EXAFS data from atoms in the first, second, and third coordination sphere and a four-shell fit (backtransform window = 1.1–3.8 Å). Numerical data for Fourier-filtered fits are contained in Table II.

(tetrahedral), as the structure deviates from  $O_h$  symmetry. The area under the pre-edge peak obtained for Co<sub>2</sub>Hr ( $5.2 \times 10^{-2}$  eV) is substantially larger than that obtained for Co(acac)<sub>3</sub> ( $3.4 \times 10^{-2}$  eV), and this difference is increased when one corrects for the ~14% increase in area expected for d<sup>6</sup> Co(III) relative to d<sup>7</sup> Co(II).<sup>23c</sup> Thus, the pre-edge analysis is also consistent with some proportion of five-coordination for the cobalt centers in Co<sub>2</sub>Hr.

**2. EXAFS.** The results of the analysis of Fourier-filtered EXAFS data from Co<sub>2</sub>Hr are summarized in Table II and Figures 5 and 6. The results of these fits were subsequently used as a starting point in the refinement of the model against the unfiltered data. The results of the fits obtained from the unfiltered data

are reported in Table III and Figure 7. The data obtained from first coordination sphere scattering atoms is fit by a single shell of four or five N,O-scatterers at an average distance of 2.12 (2) Å. This distance compares with Co–N distances of 2.16 and 2.18 Å in [Co(Im)<sub>6</sub>]CO<sub>3</sub>·5H<sub>2</sub>O,<sup>37</sup> 2.055–2.069 Å in [Co(2-MeIm)<sub>2</sub>(O<sub>2</sub>CR)<sub>2</sub>] (R = Me, *N*-Bu).<sup>38</sup> The Co–O distances for the bidentate carboxylates in the latter two structures range from 2.086

(37) Strandberg, R.; Lundberg, B. K. *Acta Chem. Scand.* **1971**, *25*, 1767–1774.

(38) Horrocks, W. D., Jr.; Ishley, J. N.; Whittle, R. R. *Inorg. Chem.* **1982**, *21*, 3270–3274.

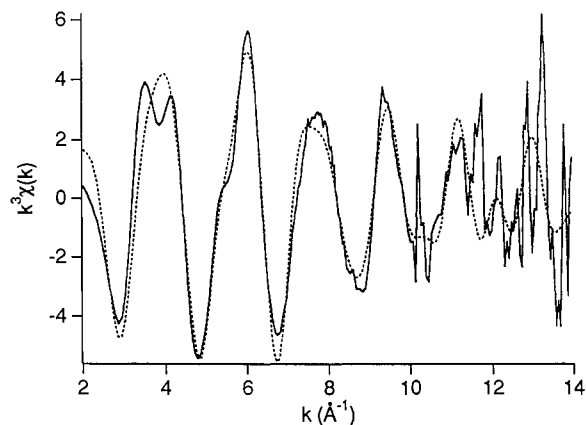


Figure 7.  $k^3$ -weighted, unfiltered EXAFS data for  $\text{Co}_2\text{Hr}$  (solid line) and a four-shell fit (dashed line). Numerical data for the unfiltered fit are contained in Table III.

Table III. EXAFS Fits Refined against Unfiltered Data for  $\text{Co}_2\text{Hr}$

no. of scattering atoms	$r$ , Å	$10^3 \Delta\sigma^2$ , Å <sup>2</sup>	$R$
5	Co-N,O = 2.116 (4)	3.0 (5)	1.56
5	Co-N,O = 2.116 (3)	2.9 (5)	1.48
1	Co-Co = 3.536 (11)	-1.0 (11)	
5	Co-N,O = 2.116 (3)	2.9 (5)	1.44
1	Co-Co = 3.537 (12)	-0.3 (11)	
1.7 (5)	Co-C = 3.051 (20)	not varied	
5	Co-N,O = 2.116 (3)	3.0 (4)	1.38
1	Co-Co = 3.525 (12)	-0.5 (11)	
1.9 (5)	Co-C = 3.052 (17)	not varied	
3.4 (8)	Co-C = 4.074 (13)	not varied	

to 2.354 Å, with an average value of 2.17 Å. Thus, Co-N<sub>HIS</sub> and Co-O<sub>carboxylate</sub> bonds, i.e., those expected for  $\text{Co}_2\text{Hr}$ , should occur at about the same distance. Similarly, in the six-coordinate complex,  $[\text{Co}(\text{CO}_3)(\text{OH}_2)(\text{Im})_2]$ ,<sup>39</sup> the Co-O<sub>carbonate</sub> bonds are 2.145 Å and the Co-N bonds are 2.112 Å and average to 2.13 Å, a distance similar to that found in  $\text{Co}_2\text{Hr}$ .

The number of first coordination sphere atoms is not well-determined from EXAFS; however, fits involving four or five first coordination sphere atoms fit the data roughly as well and better than a single shell of six N,O-donor atoms. The addition of a second independently refined shell of scattering atoms in the first coordination sphere (Table II) doubles the number of adjustable parameters from two to four, leads to a large number of highly correlated parameters, and does not substantially improve the fit. The data do not support the existence of substantially different Co-O and Co-N distances in the first coordination sphere. In particular, the addition of an O-scatterer at 1.8–1.9 Å cannot be accommodated by the data. When such a scattering atom is included in the fit, it refines to a distance of 2.10 Å, which is indistinguishable from the average distance of 2.12 Å. This result effectively rules out an oxo-bridged structure and is in contrast to EXAFS of the diiron site in various forms of metHr.<sup>2,21,27</sup> The data will not accommodate a S (Cl) scattering atom. Thus, the EXAFS analysis is completely consistent with the analysis of the UV/vis and near-IR absorption spectra in terms of five- and six-coordinate Co(II) centers with N,O-donor ligands.

The data arising from the second coordination sphere of the Co centers involve scattering arising from histidine imidazole C atoms (and possibly carboxylate C atoms) and a Co center. The features arising from these two centers are cleanly separated and leave no doubt that the peak near 2.7 Å in the Fourier-transformed spectrum (not corrected for phase shifts) (Figure 5) arises from the C scatterers, while the peak near 3.2 Å is due principally to a Co-scattering atom at a distance of  $3.54 \pm 0.03$  Å. The Fourier-filtered spectrum assigned to the Co-scattering atom

(Figure 6B) cannot be fit by a single shell of low-Z-scattering atoms and is not affected in multishell fits by the presence of second or third coordination sphere C-scattering atoms. The fit obtained for the Co-Co vector (Figure 6B) confirms that the Co atoms form a dinuclear site in the protein. The clean separation of the Co-Co vector is in contrast to EXAFS of native Hrs, where the combination of scattering arising from second coordination sphere C and Fe atoms at comparable distances often makes it impossible to unambiguously distinguish these scatterers.<sup>21,35</sup> In the absence of bridging ligands, the neighboring Co center is not expected to be detectable by EXAFS due to increases in  $\sigma^2$ , and therefore, a rigidly bridged dicobalt structure is indicated. If a single atom bridge exists, the absence of a short Co-O distance and of any scattering attributable to Cl suggests that it be a hydroxo bridge, as is found in deoxyHr.<sup>2</sup> Chaudhuri et al.<sup>11</sup> have shown by X-ray crystallography that  $[(\text{MTACN})_2\text{Co}_2(\text{OH})(\text{O}_2\text{CCH}_3)_2](\text{ClO}_4)_2 \cdot 0.5\text{H}_2\text{O}$  contains a mixed-valence ( $\mu$ -hydroxo)bis( $\mu$ -carboxylato)dicobalt(II,III) core. The Co(II)- $\mu$ -OH distance of 2.035 (12) Å in this compound is the same within experimental error as the Co-N,O distance of 2.12 (2) Å found for the first coordination shell of  $\text{Co}_2\text{Hr}$  by EXAFS. The Co-Co distance of 3.435 (4) Å in the mixed-valence compound is slightly shorter than the Co-Co distance of  $3.54 \pm 0.03$  Å found for  $\text{Co}_2\text{Hr}$ . The slightly longer Co-Co distance in  $\text{Co}_2\text{Hr}$  is consistent with the expected expansion of the dicobalt core upon reduction. A ( $\mu$ -hydroxo)bis( $\mu$ -carboxylato)dicobalt(II) core in  $\text{Co}_2\text{Hr}$  is, thus, supported by the X-ray absorption data.

The inclusion of second coordination sphere C atoms at a distance of  $\sim 3.05$  Å improves the fit to the unfiltered data (Table III) and is required in order to generate a good fit to Fourier-transformed data that includes all second and third coordination sphere scattering atoms (Figure 6C and Table II). Similarly, the peak near 3.6 Å in the Fourier-transformed spectrum (Figure 5) can be fit using a shell of C-scattering atoms at a distance of  $\sim 4.07$  Å. The second shell C atoms of imidazole ligands are expected to be located at a distance just under 1.0 Å farther than the corresponding Co-N vector.<sup>35</sup> The difference found (0.93 Å) confirms the assignment of these scatterers to second coordination sphere C atoms of histidine ligands. Additional scattering arising from third coordination sphere C and N atoms is expected for histidine ligation. The low-Z-scattering atoms found at a distance of 4.07 Å are assigned to these atoms. The distance determined is subject to large multiple scattering effects and is too short to be realistic. However, this feature and the distance involved is similar to that determined for native forms of Hr, and there is little doubt that this assignment is correct. Thus, the terminal ligands to Co in  $\text{Co}_2\text{Hr}$  are likely to consist mostly, if not totally, of imidazoles, as is the case for endogenous terminal ligands to iron in all forms of native Hr.<sup>2,27</sup>

**III. Reactivity of the Dicobalt Site.** The dicobalt site in  $\text{Co}_2\text{Hr}$  is decidedly *unreactive*, at least as monitored by vis/near-IR absorption spectroscopy. As mentioned above, no change in the absorption spectrum occurred when the protein was exposed to  $\text{O}_2$  or sodium dithionite at pH 7. Treatment of  $\text{Co}_2\text{Hr}$  with up to 40-fold molar excesses of hydrogen peroxide or ferricyanide also failed to significantly perturb the absorption spectrum even after several hours of reaction at room temperature. Furthermore, the absorption spectrum was found to be independent of pH between 6.0 and 8.8 and was unperturbed by extensive dialysis of  $\text{Co}_2\text{Hr}$  against 100 mM sodium azide at pH 7 and 4 °C.

While the lack of reactivity with  $\text{O}_2$  is not unusual for Co(II) substituted into proteins,<sup>29</sup> it must also be noted that the other two known  $\text{O}_2$ -carrying proteins, namely, hemocyanin and hemoglobin, have both been reported to form  $\text{O}_2$  adducts when cobalt is substituted for the native metals.<sup>40,41</sup> However, distinct differences exist between the Co sites in both of these other proteins and that in  $\text{Co}_2\text{Hr}$ . In the case of cobalt-substituted hemoglobin,

(39) Baraniak, E.; Freeman, H. C.; James, J. M.; Nockolds, C. E. *J. Chem. Soc. A* 1970, 2558–2566.

(40) Hoffman, B. M.; Petering, D. H. *Proc. Nat. Acad. Sci. U.S.A.* 1970, 67, 637–643.

(41) Dutton, T. J.; Baumann, T. F.; Larrabee, J. A. *Inorg. Chem.* 1990, 29, 2272–2278.

the most obvious difference is incorporation of Co(II) into a porphyrin, which leads to a low-spin state for Co(II).<sup>31</sup> Many similar mononuclear low-spin Co(II) complexes bind O<sub>2</sub> reversibly.<sup>42</sup> The O<sub>2</sub> adduct in cobalt-substituted hemocyanin is formulated as a ( $\mu$ -hydroxo)( $\mu$ -peroxo)dicobalt(III) complex, which represents the other known structural type resulting from reaction of synthetic Co(II) complexes with O<sub>2</sub>.<sup>42,43</sup> In contrast to the dicobalt site in Co<sub>2</sub>Hr, the visible absorption spectrum of cobalt-substituted hemocyanin prior to exposure to O<sub>2</sub> indicates that the active-site Co(II) have a pseudotetrahedral coordination geometry and that these Co(II) centers are accessible to solvent and exogenous ligands.<sup>41</sup> If a ( $\mu$ -hydroxo)bis( $\mu$ -carboxylato)dicobalt(II) core accurately describes the complex in Co<sub>2</sub>Hr, then access of O<sub>2</sub> to both Co centers simultaneously is likely to be severely inhibited, as is the case for the diiron(II) site in native deoxyHr.<sup>2</sup> Thus, the dimetal site favored in Hr is not designed to accommodate either known type of adduct resulting from reaction of Co(II) with O<sub>2</sub>.<sup>42,43</sup> In addition, the lack of a pH-dependent absorption spectrum and of azide binding noted above suggest a general inaccessibility of small molecules to the dicobalt site in Co<sub>2</sub>Hr, despite the five-coordinate Co(II) indicated by the spectroscopic data. The diferrous site in deoxyHr also shows no evidence for interaction with solvent but does show evidence for complex formation with azide.<sup>45</sup>

### Summary and Conclusions

A simple method is described for high-yield preparation of a cobalt-substituted Hr. The cobalt-substituted Hr closely resembles

the native protein in polypeptide helix content and molecular weight, indicating that the protein subunit structure and inter-subunit interactions have been preserved. Close to 2 Co/Hr subunit with no detectable iron is reproducibly obtained, suggesting that cobalt occupies the same coordination sites as iron in the native protein. Analysis of the EXAFS data provides proof of a dicobalt site (3.54-Å Co-Co distance) with histidine ligation. The requirement of correlated motion of the Co scatterers for observation of EXAFS implies the existence of one or more bridging ligands. Given the single distance (2.12 Å) found for the first coordination sphere donor atoms, and comparisons to synthetic complexes, a hydroxo bridge is suggested. The X-ray absorption as well as the UV/vis and near-IR absorption and CD spectra indicate that all of the cobalt in Co<sub>2</sub>Hr is in the +II oxidation state, even in air, that the coordination spheres consist exclusively of N,O-donor ligands, and that both five- and six-coordinate Co centers are present in significant proportions. Given the five- and six-coordinate iron centers with terminal histidine ligands in the ( $\mu$ -hydroxo)bis( $\mu$ -carboxylato)diiron(II) site of deoxyHr, an isostructural dicobalt(II) site is strongly suggested in Co<sub>2</sub>Hr. The absorption spectrum of the dicobalt(II) site in Co<sub>2</sub>Hr is unaffected by variations in pH or by the presence of azide, O<sub>2</sub>, or H<sub>2</sub>O<sub>2</sub>. Apparently, even the five-coordinate Co center is inaccessible to solvent and exogenous ligands. Despite this lack of reactivity, the close structural analogies to native Hr and the stability of Co<sub>2</sub>Hr are likely to facilitate studies of the relationship between protein folding and dimetal site assembly. This relationship will be addressed subsequently.<sup>46</sup>

**Acknowledgment.** This research was supported by NIH Grants GM40388 (D.M.K.) and GM38829 (M.J.M.). The near-IR CD/MCD spectrometer was purchased with funds from an NSF Research Training Group Award to the Center for Metalloenzyme Studies (DIR 9014281). We thank Gerald J. Colpas and Csaba Bagyinka for help in collecting the X-ray absorption spectra. We thank Michael K. Johnson for helpful discussions regarding the near-IR absorption and CD of Co<sub>2</sub>Hr.

- (42) Cotton, F. A.; Wilkinson, G. *Advanced Inorganic Chemistry*, 5th ed.; Wiley-Interscience: New York, 1988; pp 735-738.  
 (43) A recently described side-on bonded superoxo complex of Co(II) results from reaction of a formally Co(I) complex with O<sub>2</sub>.<sup>44</sup>  
 (44) Egan, J. W., Jr.; Haggerty, B. S.; Rheingold, A. L.; Sendlinger, S. C.; Theopold, K. H. *J. Am. Chem. Soc.* **1990**, *112*, 2445-2466.  
 (45) (a) Maroney, M. J.; Kurtz, D. M., Jr.; Nocek, J. M.; Pearce, L. L.; Que, L., Jr. *J. Am. Chem. Soc.* **1986**, *108*, 6871-6879. (b) Wilkins, P. C.; Wilkins, R. G. *Biochim. Biophys. Acta* **1987**, *912*, 48-55. (c) Reem, R. C.; Solomon, E. I. *J. Am. Chem. Soc.* **1987**, *109*, 1216-1226. (d) Hendrich, M. P.; Pearce, L. L.; Que, L., Jr.; Chasteen, N. D.; Day, E. P. *J. Am. Chem. Soc.* **1991**, *113*, 3039-3044.

- (46) Zhang, J.-H.; Kurtz, D. M., Jr. Manuscript in preparation.

Contribution from the Department of Chemistry, Box CH, Mississippi State University, Mississippi State, Mississippi 39762

## Infrared and <sup>13</sup>C and <sup>15</sup>N NMR Studies of Cyano(ligand)cobaloximes: Evidence for Cobalt-to-Cyanide $\pi$ -Bonding

Kenneth L. Brown\* and S. Satyanarayana

Received July 19, 1991

A series of 17 cyano(ligand)cobaloximes have been prepared, including 6 with 4-substituted pyridine ligands, 6 with primary amine ligands, 3 with 4-substituted aniline ligands, the ammonia complex, and the potassium salt of the thiocyanato complex. The analogous series of complexes enriched in <sup>13</sup>C and <sup>15</sup>N in the cyanide ligand have been used to locate the cyanide <sup>13</sup>C and <sup>15</sup>N NMR resonances and the cyanide stretching frequencies in the infrared spectra. As the trans axial ligand is varied, an inverse dependence of the <sup>15</sup>N chemical shifts on the <sup>13</sup>C chemical shifts is observed, and for 14 of the complexes the chemical shift data give an excellent linear correlation with a slope of -0.614. These data, together with trends in  $\delta_{15N}$ ,  $\delta_{13C}$ , and  $\nu_{CN}$  with the basicity of the trans axial ligand, are interpreted to indicate that cobalt-to-cyanide  $\pi$ -bonding is important in these cyanocobalt complexes.

### Introduction

In a recent report,<sup>1</sup> a curious inverse dependence of the <sup>13</sup>C and <sup>15</sup>N NMR chemical shifts of cyanide ion bound to cobalt corrins upon changes in inner-sphere coordination was observed. Thus, conversion of the base-on form of cyanocobalamin to the base-off form (in which the dimethylbenzimidazole ligand is replaced by

water) caused a 9.6 ppm upfield shift of the cyanide <sup>13</sup>C resonance but a 8.7 ppm downfield shift of the <sup>15</sup>N resonance. In contrast, protonation of CN<sup>-</sup> causes an upfield shift of both the <sup>13</sup>C and <sup>15</sup>N resonances (by 52.4 and 26.9 ppm, respectively) as expected.<sup>1</sup> Similarly, for eight cobalt corrin-bound cyanide species in various coordination environments, a reasonably good ( $r^2 = 0.89$ ) linear correlation of  $\delta_{15N}$  with  $\delta_{13C}$  with a slope of -0.73 was found to exist. This correlation not only confirms the inverse behavior of the <sup>13</sup>C and <sup>15</sup>N cyanide chemical shifts of cyanocobalt corrins

(1) Brown, K. L.; Gupta, B. D. *Inorg. Chem.* **1990**, *29*, 3854.